Novel resolution pathways in liver ischemia and reperfusion injury

N. Xia, T. Huey, C. Zhong, T. Morinelli, S. Hanish, Y. Zhai, Transplant Surgery, Medical University of South Carolina, Charleston, SC



ABSTRACT

The mechanism of inflammation resolution is a major unresolved issue in the research of liver ischemia reperfusion injury (IRI). We took advantage of newly developed mouse models to study the dynamic interaction of liver resident Kupffer cells (KCs) and monocyte-derived infiltrating macrophages (moMφ) in liver IRI. In a murine model of liver partial warm IR, we traced the fate of KCs and moMøs in Clec4F-tdTomato and CCR2-GFP mice. To facilitate the delineation of cellular mechanisms of inflammation resolution, we also employed zymosan-induced peritonitis model (ZIP, 10ug, i.p.). In Clec4F-tdTomato mice, we found that resident KCs (Clec4F+F4/80+CD11blow) were significantly depleted at 6h post reperfusion when liver IRI was peaked, in parallel with the infiltration of moMøs. At day 7 post IR, hepatocellular injuries were mostly repaired. Resident KCs were recovered, and they were mostly derived from the original embryonic KCs (TIM-4+) via self-proliferation with minimal contribution of moMos (TIM-4-). Thus, moMo contraction might represent a main resolution mechanism in liver IRI. In CCR2-GFP mice, moMøs were GFP+ and none of them were detected in the recovered KC population. In the ZIP model, similar dynamic changes of macrophage subsets were detected: peritoneal resident M\u00f3s (TIM-4+) were reduced, with simultaneous infiltrations of moM\u00f4s at the activation phase (at 4-12h post Zymosan injection). In the resolution phase (24h-7days), recovered resident Mos were all TIM-4+ and no GFP+CCR2+ moMos became TIM-4+. FACS analysis detected consistent low percentages of apoptotic (annexin V+) moMφs (TIM-4-), in parallel with GFP+ resident Mφs (TIM-4+) at comparable percentages. Image flowcytometry showed that resident Mos indeed engulfed GFP+ moMos. In vitro coculture experiment confirmed that TIM-4+ resident Mos from non-GFP sham mice were able to engulf TIM-4-moMos from the GFP ZIP mice. Furthermore, gene expression analysis (qRT-PCR) showed that moMos in the resolution phase downregulated anti-apoptotic Bcl-2 but upregulated pro-apoptotic Bim expression. These results indicate that the restoration of liver macrophage homeostasis in liver IRI involves both the recovery of resident KCs via self-proliferation, as well as the contraction of infiltrating moMøs. Efferocytosis of apoptotic moMøs by tissue resident Møs may constitute a novel pathway in the inflammation resolution. A better understanding of these novel mechanisms may provide us new therapeutic strategies to alleviate IRI in liver Tx.

METHODS

Mouse liver partial warm ischemia model. After a midline laparotomy, mice were injected with heparin (100 μg/kg) and an atraumatic clip was used to interrupt arterial/portal venous blood supply to the cephalad-liver lobes. After 60 min of ischemia, the clip was removed to initiate hepatic reperfusion. Sham controls underwent the same procedure, but without vascular occlusion. Mice were sacrificed after 6h to 7 days of reperfusion, and liver and serum samples were collected. Serum alanine aminotransferase (sALT) levels were measured.

Isolation of Liver Non-Parenchymal Cells (NPCs) Livers were perfused in situ via the portal vein with ice-cold PBS to remove circulating blood. After perfusion, livers were excised, minced into small pieces, and transferred into a digestion buffer containing Collagenase IV (0.5 mg/mL) and DNase I (40 μg/mL). The tissue suspension was incubated at 37°C for 30 minutes in a water bath with gentle agitation. Following enzymatic digestion, the cell suspension was passed through a 40 μm cell strainer to remove debris and undigested fragments. The filtrate was centrifuged at 50 × g for 5 minutes at 4° C to pellet hepatocytes, and the supernatant containing non-parenchymal cells was collected. To further enrich NPCs, the supernatant was centrifuged at 500 × g for 5 minutes, followed by red blood cell lysis using RBC lysis buffer. Cells were then washed and centrifuged again to obtain the NPC pellet, which was resuspended in FACS buffer for flow cytometry analysis.

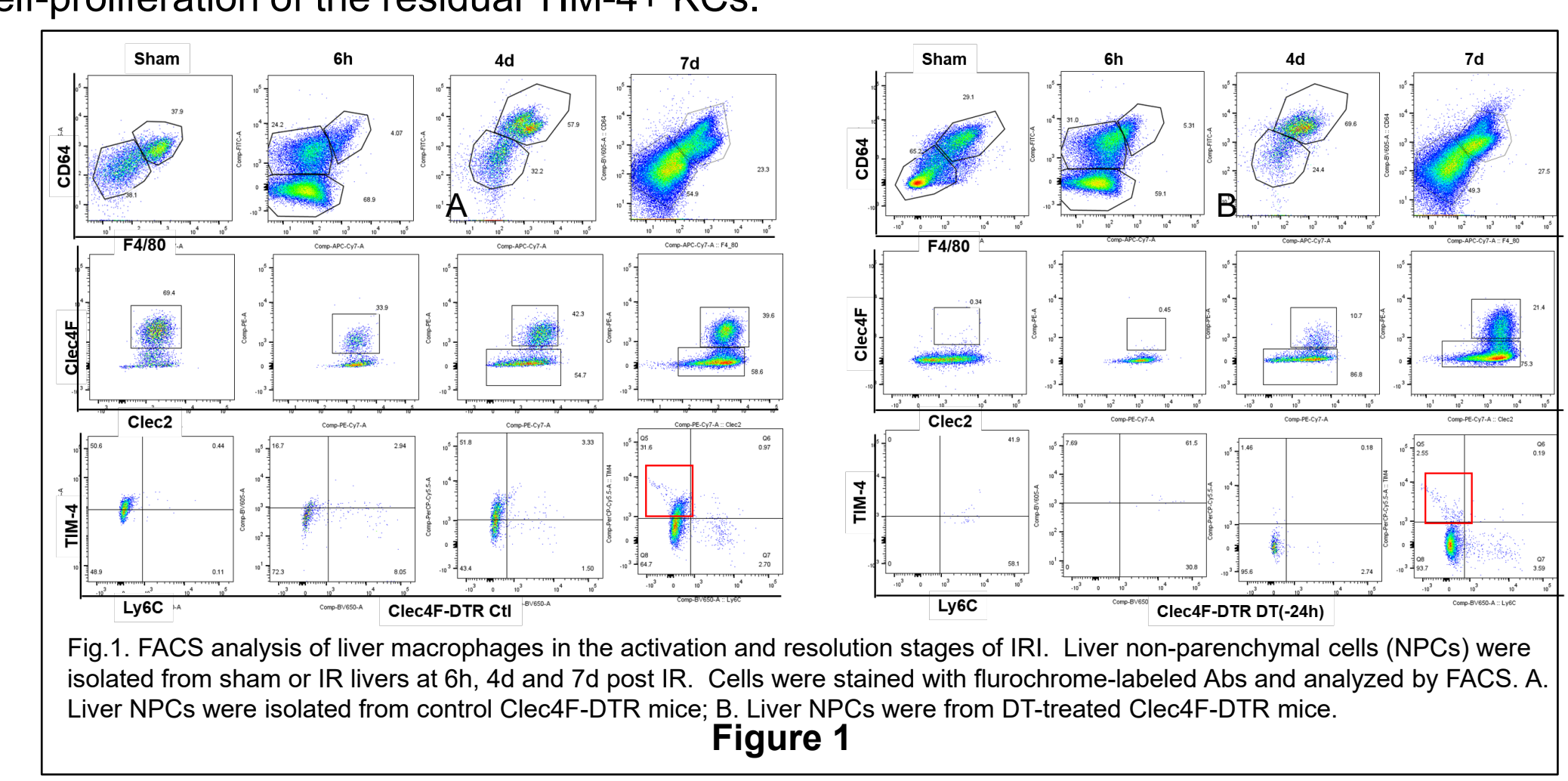
Macrophage Depletion. To deplete KCs or CD11b+ infiltrating macrophages, we injected diphtheria toxin at 10 □g/g mouse body weight, i.v. 24h prior to the onset of liver ischemia. The selective depletion of KCs and CD11b macrophages in these mouse models as confirmed by FACS analysis of liver non-parenchymal cells and peritoneal exudes 24h post DT injection. As shown in Sup Fig.1, KCs (F4/80+Clec4F+TIM4+) were depleted in Clec4F-DTR, but not CD11b-DTR mice, while peritoneal macrophages (F4/80+CD11b+) were depleted in CD11b-DTR, but not Clect4F-DTR mice.

Flowcytometry 1 × 10⁶ cells were first incubated with rat anti–mouse CD16/32 for 10 minutes, followed by staining with rat anti–mouse F4/80, CD11b, Ly6G, Clec4F, TIM-4, MerTK, or isotype-matched control Ab for 20 minutes. Cells were washed with PBS and subjected to flow cytometry analysis with BD LSR Fortessa (BD Biosciences).

RESULTS

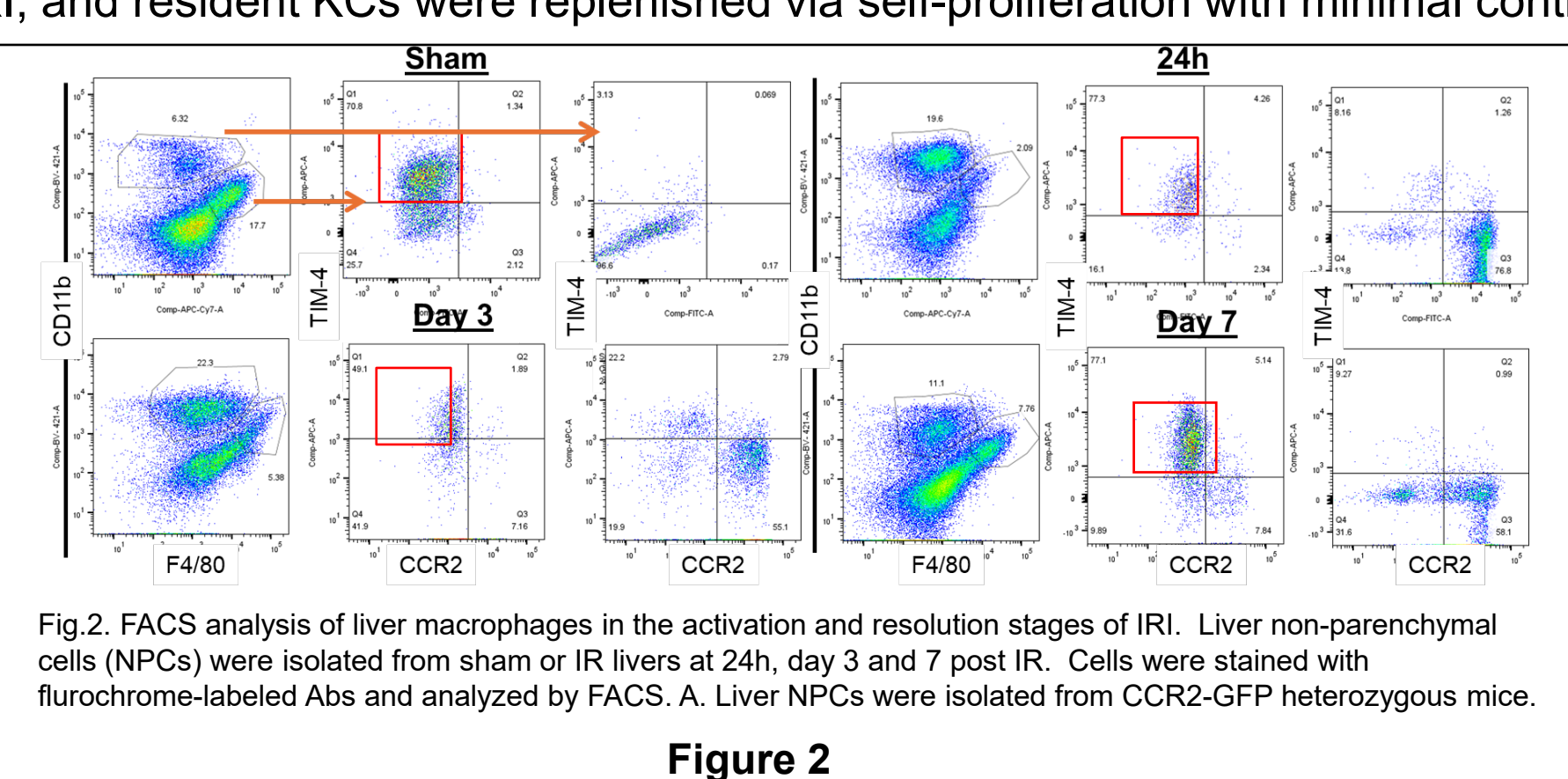
1. KCs are recovered by self-proliferation, not conversion from infiltrating macrophages in liver IRI.

Liver NPCs were isolated from sham or IR livers at 6h, 4 days and 7 days post IR in two cohorts of Clec4F-DTR mice treated with either PBS (Ctl) or DT at 24h prior to the onset of liver ischemia. Cells were stained with fluorochrome-labeled Abs and analyzed by FACS (Fig.1A). CD45+ cells were gated and further separated into macrophage and non-macrophage populations based on F4/80 and CD64 expression. Macrophages (F4/80 and CD64 double positive) were then divided into KCs and non-KCs based on Clec2 and Clec4F (tdTomato⁺). Finally, TIM-4 expression was measured in KCs. In sham liver, approximately 50% of KCs were TIM-4⁺. Liver IR depleted this KC population significantly (at 6h post IR): % of macrophages in CD45 cells was decreased to 4% (vs. 37% in sham) and % of KCs in macrophages and TIM-4+ KCs were also decreased. During the recovery stage of liver IRI at day 4 and 7 post IR, % of macrophages in liver CD45+ cells was restored. Although % of KCs was lower in macrophages, % of TIM-4+ KCs was back to the same levels in sham controls. KC recovery can be mediated by two potential mechanisms, self-proliferation and conversion from infiltrating macrophages. To differentiate these two possibilities, we analyzed KC recovery in DT-treated Clec4F-DTR mice (Fig.1B). A single dose of DT completely depleted TIM-4+ KCs in the liver (sham). Livers were repopulated with infiltrating macrophages negative for both Clec4F and TIM-4. Liver IR similarly depleted macrophages at 6h. When IR livers were recovered (7d), Clec4F+ KCs are partially restored. However, they were all TIM-4⁻. This result indicates that infiltrating macrophages were not converted to TIM-4+ KCs during the recovery stage of liver IRI. Thus, recovered TIM-4+ KCs (in Clec4F-DTR mice w/o DT treatment) are derived from self-proliferation of the residual TIM-4+ KCs.



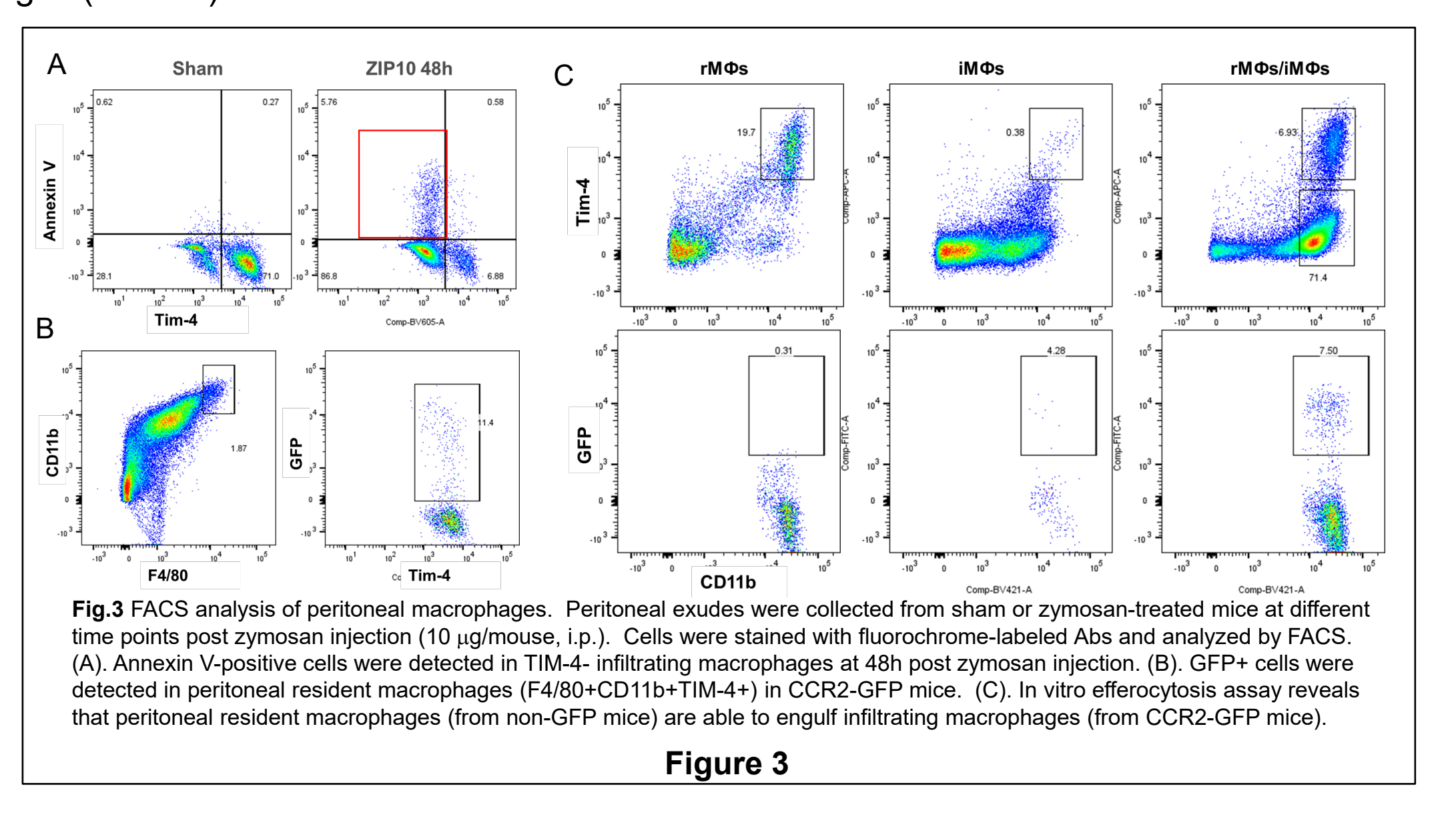
2. CCR2+ infiltrating macrophages were not converted to KCs in liver IRI

To determine whether infiltrating macrophages are converted to KCs when liver IRI is resolved, we used CCR2-GFP heterozygous mice in the liver IRI experiment (Fig.2). In sham livers, all KCs (TIM-4+F4/80+CD11blow) were GFP-. At 24 hours and day 3 post-IR, residual KCs remained GFP-, moMΦs (F4/80lowCD11b+) were predominantly GFP+. At day 7, KCs were mostly recovered and no GFP+ cells were detected in KCs. Meanwhile both CCR2+ and CCR2- infiltrating cells remained present in the liver, which were all TIM-4-. These results suggest that CCR2+ moMΦs do not convert to KCs during the recovery stage of liver IRI, and resident KCs were replenished via self-proliferation with minimal contribution from moMΦs.



3. Infiltrating macrophages become apoptotic and are cleared by resident macrophages via efferocytosis

To facilitate our analysis of the dynamic changes of resident vs. infiltrating macrophages, we used zymosan-induced peritonitis (ZIP, $10\mu g$, i.p.) model. To determine whether infiltrating macrophages were contracted at the resolution stage of the inflammation, we collected peritoneal exudes at 24 and 48h post zymosan injection. Indeed, low levels (~5%) of Annexin V+ cells were consistently detected (Fig.3A) selectively in the infiltrating macrophages (TIM-4-) but not (or at significantly lower levels) in the resident macrophages (TIM-4+).



TIM-4 is a universal marker of tissue resident macrophages and not expressed in infiltrating macrophages (Ly6C+) at the activation stage of inflammation. TIM-4 is induced in reprogrammed infiltrating macrophages (Ly6C-) at the late stage of inflammation resolution (>48h, up to 7 days) in the ZIP model. Interestingly, in CCR2-GFP heterozygous mice, we have detected TIM-4+ GFP+ cells at all time points after zymosan injection (Fig.3B). To distinguish whether they were converted from CCR2 infiltrating cells or TIM-4+ resident which had engulfed CCR2 infiltrating macrophages, we employed image flow cytometry. As shown in Fig.4, in the single cell population, we did find GFP+TIM-4+ cells. GFP was clearly inside of TIM-4+ cells as puncta of different sizes, indicating that resident macrophages did engulf GFP+ infiltrating macrophages. As controls, we also analyzed doublet cell population. There were GFP+ cells in close contact with TIM-4+ cells. We did not detect any GFP+ cells converted to TIM-4 positive (universal green with surface red cells).

To confirm that resident macrophages are capable of engulfing infiltrating macrophages, we performed co-culture experiments in vitro. Resident macrophages were isolated from non-CCR2-GFP sham mice and infiltrating macrophages from CCR2-GFP mice (48h post 100µg zymosan injection which depletes all resident macrophages). After 2h coculture, cells were labeled with fluorochrome labeled anti-CD11b, TIM-4 and analyzed by FACS. Approximately 7% of CD11b+TIM-4+ cells became GFP+ after the co-culture (Fig.3C). The relatively small % of GFP+ resident macrophages in the in vitro experiment was consistent with those detected in vivo. Thus, in the resolution of the peritoneal inflammation, infiltrating macrophages do become apoptotic and cleared by resident macrophages via efferocytosis. The relatively low percentages of apoptotic infiltrating macrophages and efferocytotic resident macrophages are indicative of a slow process of the restoration of macrophage homeostasis (>7 days).

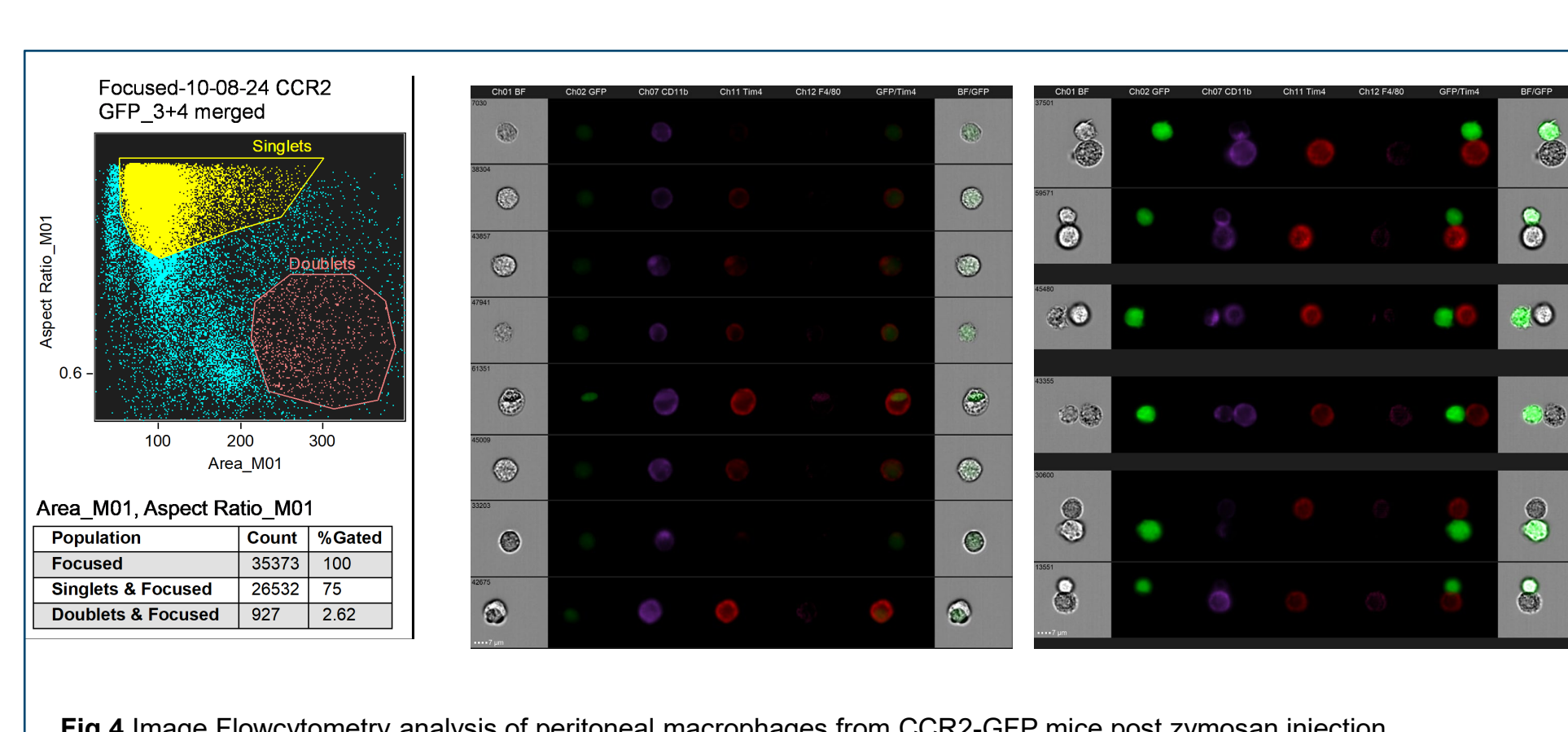
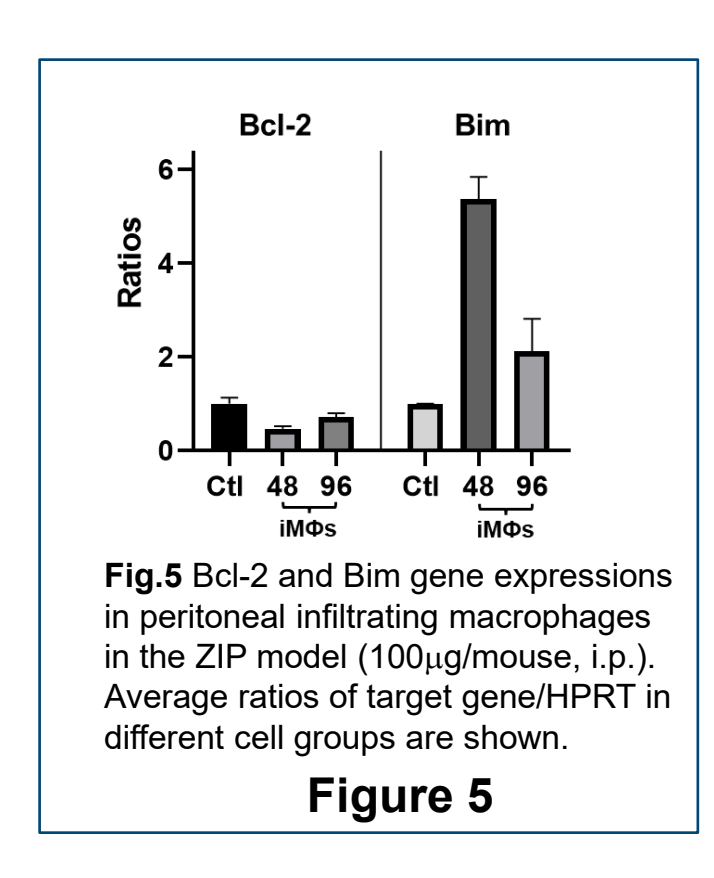


Fig.4 Image Flowcytometry analysis of peritoneal macrophages from CCR2-GFP mice post zymosan injection. Peritoneal exudes were collected from zymosan-treated mice(10 μg/mouse, i.p.) at 48h post injection. Cells were stained with PE-anti-TIM-4, BV421-anti-CD11b and analyzed by ImageStream ISx. The dot plot shows the gates of singlet and doublet cells. The middle panel shows representative single cell images and the left panel shows cell images of doublets.

Figure 4

Finally, we analyzed the expression of antiapoptotic gene Bcl-2 and pro-apoptotic gene Bim in infiltrating macrophages in the resolution phase (48h and 96h after zymosan injection) as compared with resident macrophages (sham) by qRT-PCR (Fig.5). Clearly, Bcl-2 levels were decreased while Bim levels were increased in infiltrating macrophages, supportive of apoptosis induction.



CONCLUSIONS

- Kupffer cells are severely depleted during the acute phase of liver ischemia-reperfusion injury (IRI) and are gradually restored during the resolution.
- Kupffer cell restoration is mainly dependent on their selfrenewal, not infiltrating macrophage conversion.
- Infiltrating macrophages do not convert to resident macrophages during the resolution phase of peritoneal inflammation. They become apoptotic and are eliminated via efferocytosis by resident macrophages.

ACKNOWLEDGMENT

The work is supported by NIH grant 1R01DK119338, 2P01Al120944 and Research Fund from Medical University of South Carolina.